Image Registration Techniques Alter Image Properties in fMRI

Kevin K. Liu[1] and Daniel B. Rowe[1,2]
[1]Department of Mathematics, Statistics and Computer Science, Marquette University, Milwaukee, WI, USA
[2]Department of Biophysics, Medical College of Wisconsin, Milwaukee, WI, USA

Abstract

Functional Magnetic Resonance Imaging (fMRI) is a non-invasive means to determine active parts of the brain by observing changes in the Blood Oxygen Level Dependent (BOLD) signal. The reconstruction pipeline of the complex-valued *k*-space data often coincides with multiple image processing techniques. Implemented both before and after the actual reconstruction, image processing enhances the overall quality or a particular aspect of an image. Registration is an important processing step out of many others included in the fMRI reconstruction pipeline, which can be described as the alignment of two or more images through geometric transformations. It has been shown in recent studies that some image processing operations can alter the statistical properties of an image and even induce artificial correlation of non-biological origins between voxels. This concept applies to common fMRI registration algorithms as well, the extent and structure of these effects will be examined. Quantifying any potentially induced correlation from image registration can allow for future development of statistical models that will greatly improve the accuracy and reliability of fMRI studies.

1. Introduction

The emergence of projects such as the Human Connectome Project have provided a source of readily available experimental fMRI data. The large database of easy access data has become an essential resource for many researchers. However, this has also lead to the unknowingly careless use of data sets without regard to the processing that has been performed. In essence creating a black box complex-valued (CV) reconstruction pipeline from data acquisition to analysis. In actuality, multiple steps are performed before any image analysis is performed. This includes pre-processing (e.g. Nyquist ghost correction, zero-filling, apodization, etc.), reconstruction depending upon acquisition method (e.g. Cartesian acquisition, spiral acquisition, parallel acquisition, etc.), and post-processing (e.g. smoothing, sharpening, slice timing correction, registration, etc.).

Image registration is an important and in many cases a necessary processing step included in the CV reconstruction pipeline. The registration of intra-subject and inter-subject studies are necessary for any meaningful analysis. Especially important when movement or anatomical differences are significant factors that need to be accounted for. It is a great example of an algorithm not limited to only fMRI and is used in accordance with a variety of medical imaging modalities.

1.1. Motivation

It has recently been shown that some image processing techniques can alter the statistical properties of an image. It is possible to induce both spatial and temporal correlations between voxels of no biological origin. These induced correlations can either be local or far reaching in structure or compound upon each other with the combination of multiple processing techniques. A simple estimate of these altered statistical properties can be obtained with time consuming and computationally intensive Monte Carlo simulations. However, estimates formulated from Monte Carlo methods are naturally noisy and do not provide the necessary accuracy.

The widespread and sometimes automatic implementation of image registration algorithms calls for an accurate understanding of the potential statistical effects. Instead of Monte Carlo simulations, a linear framework model will be used to accurately describe any changes in statistical properties of an image. The model will display the statistical effects of image registration implemented independently and in correspondence with other image processing techniques. Variations in analysis results of activation and connectivity will emphasize that the aftereffects of an image processing algorithm is equally important to the results it produces.

2. Background

2.1. Complex-Valued Reconstruction Pipeline

In fMRI, a time series of complex-valued (CV) data is collected in the spatial frequency domain, *k*-space, given some acquisition method. The simplest method is a Cartesian sampling in *k*-space which is then reconstructed through a 2-dimensional inverse Fourier transformation. Other methods such as spiral or parallel acquisitions are faster but have a more involved reconstruction process and side effects (spiral causes blurring).

In addition to the reconstruction algorithm of the complex-valued data, a number of image processing techniques are implemented before and after. For the sake of consistency between different research fields, processing done before and after reconstruction will be referred to as pre-processing and post-processing, respectively. Both pre-processing and post-processing steps in the CV pipeline are made up of the application of multiple mathematical algorithms which greatly enhance an image's quality. Pre-processing operations are generally necessary before any reconstruction, and can vary dependent upon the CV data acquisition and reconstruction method. Post-processing is performed to further enhance the analysis results.

The CV reconstruction pipeline can be constructed from a large set of combinations of pre-processing, reconstruction, and post-processing algorithms. The inclusion or exclusion of a particular algorithm in any

of the steps or the interchanging of the order of two operations could greatly alter the resulting properties of a reconstructed image before analysis. It should be emphasized that there is an incredible amount of variability in the CV reconstruction and processing pipeline at each step and as a whole.

2.2. Image Registration

Image registration can be described as the alignment of one or more images to a template through geometric transformations. Most fMRI registration algorithms can be simplified into two stages: (1) an optimization with respect to some pre-determined cost function to find a suitable geometric transformation [6.7], and (2) an interpolation is implemented for non-integer voxel coordinates [1,2].

Registration itself is a rather extensive topic and is made up of a multitude of methods which exist for different scenarios; for example, the registration of inter-subject as opposed to intra-subject images can vary greatly in computational intensity and methodology. In addition, several popular fMRI processing and analysis software packages exist, each with its' own image registration algorithm, such as FSL, SPM, and AFNI. The algorithms in the various packages share several similarities, but there is no established standard algorithm for image registration. These variabilities will produce slightly different registration results for the same image between different software packages, but all packages and their algorithm adhere to the same idea. Decisions on the choice of the algorithm determination should be a made on a case by case basis.

In digital image processing, an image can be geometrically transformed (warp, shift, scale, etc.) multiple ways [3,4]. One of them is to define the geometric transformation as a linear set of equations which also form a transformation matrix, Eq. 1. This same method is applied in most fMRI registration algorithms. A 3-dimensional transformation can include up to 12 different parameters: 3 rotation, 3 scaling, 3 shearing, and 3 shifting parameters. The parameters are optimized with respect to some cost function [7]. Differing image registration algorithms will vary in number of parameters, optimization methods, and cost functions (e.g. mean squared error, mutual information, correlation ratio, etc.).

Following the geometric transformation, each voxels' respective coordinates may no longer adhere to a grid of integer values. An interpolation scheme is implemented to account for the non-integer voxel coordinates (e.g. nearest neighbor interpolation, bi-linear interpolation, sinc interpolation, etc.).

2.3. A Linear Framework

Monte Carlo simulations are a useful method to estimate the statistical properties of an image. However, the naturally noisy results are still produced and this leaves an unnecessary amount of inaccuracy. It can be reduced but not eliminated with large and time consuming simulations; Instead, the use of a linear framework model can more accurately depict the statistical properties of an image [8,9]. This linear framework will take advantage of some basic matrix properties, Eq.1.

Given a vector f of dimension $N^2 \times 1$ with $\mu_f = E(f)$ and $\Sigma_f = cov(f)$, and a matrix O of dimension $N^2 \times N^2$. If, Eq. 1

$$v = O \times f$$

then,

$$\mu_v = E(v) = O \times \mu_f \text{ , } \Sigma_v = \mathrm{cov}(v) = O \times \Sigma_f \times O^T \text{ , and } \rho_v = corr(v) = D^{-1/2} \times \Sigma_v \times D^{-1/2}$$

where, D is a square matrix of the diagonal elements of the covariance matrix Σ_f

Usually, image processing techniques in fMRI are mathematically computed as a convolution operation. In this linear framework, convolution will be represented differently to fulfill Eq. 1. The

convolution operation itself can be understood in several different ways: (a) The iterative process of a mask or kernel overlayed the original image, (b) with some matrix reshaping, a matrix multiplication in image space, (c) and using the Fourier convolution theorem, a matrix multiplication in frequency space. These three methods are graphically displayed in, Figs 1 (a) – (c).

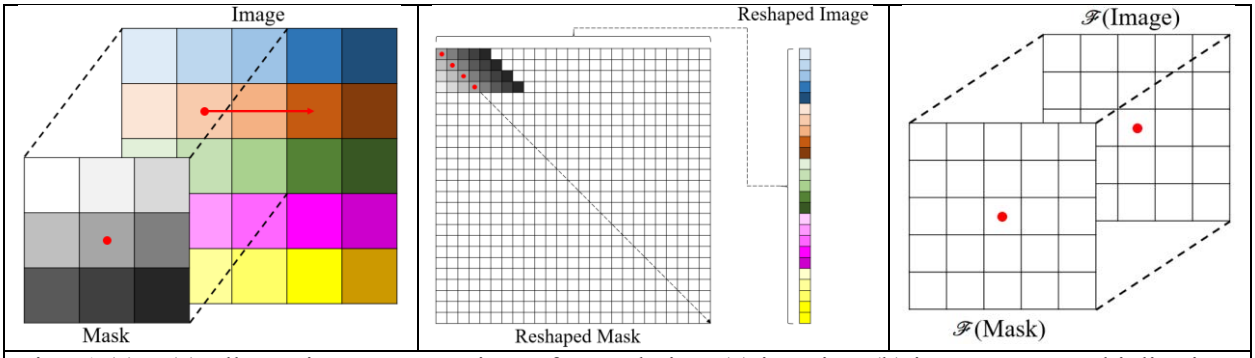

Figs. 1 (a) – (c). Illustrative representations of convolution: (a) iterative, (b) image space multiplication, and (c) frequency space multiplication.

Given Eq. 1 and the conversion from an iterative sequential voxel process to a global simultaneous matrix multiplication in image space, if the mean and covariance of the original image are known, then the mean and covariance after multiplication can be found as well. The mathematical descriptions for both methods are displayed in, Eq. 2 & Eq. 3 respectively. You don't say what you do at the image edges.

$$(g * f)(x,y) = \sum_{i=1}^{M}\sum_{j=1}^{M}[g(i,j)f(x-(M-i),y-(M-j))] \qquad \text{Eq. 2}$$

Where g is an $M \times M$ convolution mask and f is an $N \times N$ image.

$$f' = \begin{bmatrix} f(1,1) \\ f(1,2) \\ \vdots \\ f(2,1) \\ f(2,2) \\ \vdots \\ f(N,N) \end{bmatrix} \quad \& \quad O = \begin{bmatrix} g(i,j) & g(i,j+1) & \cdots & g(M,M) & & \\ g(i,j-1) & g(i,j) & g(i,j+1) & \cdots & g(M,M) & \\ & & & & & \\ & & & & \ddots & \\ & & & & & g(i,j) \end{bmatrix}, \begin{matrix} i = j = \frac{M+1}{2}, M \bmod 2 = 1 \\ i = k = \frac{M}{2}, M \bmod 2 = 0 \end{matrix} \qquad \text{Eq. 3}$$

$$(g * f)(x,y) = O \times f'$$

Where O is an $N^2 \times N^2$ matrix operator representing the reshaped convolution mask and f' is an $N^2 \times 1$ vector representing the reshaped image.

2.4. Illustrative Example

An illustrative example will better display this conversion of convolution from an iterative sequential voxel process to a global simultaneous matrix multiplication in image space as well as confirm that both produce identical results. This example will first use a generic matrix and convolution kernel, Ex. 1, then the formation of a matrix operator of the 2-dimensional discrete inverse Fourier transform, Ex. 2.

Given a function $f(x,y)$ and convolution kernel $g(x,y)$ where (x,y) represent the spatial locations, Ex. 1

$$f(x,y)=\begin{bmatrix} f(x_1,y_1) & f(x_1,y_2) \\ f(x_2,y_1) & f(x_2,y_2) \end{bmatrix} \;\&\; g(x,y)=\begin{bmatrix} g(x_1,y_1) & g(x_1,y_2) \\ g(x_2,y_1) & g(x_2,y_2) \end{bmatrix}$$

If using Eq. 2,

$$(g*f)(x,y)=\begin{bmatrix} g(x_1,y_1) & g(x_1,y_2) \\ g(x_2,y_1) & g(x_2,y_2) \end{bmatrix} * \begin{bmatrix} f(x_1,y_1) & f(x_1,y_2) \\ f(x_2,y_1) & f(x_2,y_2) \end{bmatrix}$$

$$(g*f)(x,y)=g(x_1,y_1)f(x_1,y_1)+g(x_1,y_2)f(x_1,y_2)+g(x_2,y_1)f(x_2,y_1)+g(x_2,y_2)f(x_2,y_2)$$

Then using Eq. 3,

$$(g*f)(x,y)=\begin{bmatrix} g(x_1,y_1) & g(x_1,y_2) & g(x_2,y_1) & g(x_2,y_2) \end{bmatrix} \begin{bmatrix} f(x_1,y_1) \\ f(x_1,y_2) \\ f(x_2,y_1) \\ f(x_2,y_2) \end{bmatrix}$$

$$(g*f)(x,y)=g(x_1,y_1)f(x_1,y_1)+g(x_1,y_2)f(x_1,y_2)+g(x_2,y_1)f(x_2,y_1)+g(x_2,y_2)f(x_2,y_2)$$

With respect to the 2-dimensional inverse Fourier transformation, the acquired *k*-space is a function of proton spin density and the accumulated phase with respect to time and acquisition method. This formulation leads to the Fourier relationship from *k*-space to image space and the rational for the reconstruction method. A matrix operator representation of the Fourier transformation is an integral part of this linear framework.

Given a *k*-space acquisition $f(x,y)$ of dimension $N\times N$ it can be reshaped as $2N^2\times 1$ where (x,y) represent the spatial locations, Ex. 2

$$f(x,y)=\begin{bmatrix} f_{real}(x_1,y_1) \\ \vdots \\ f_{real}(x_N,y_N) \\ f_{imaginary}(x_1,y_1) \\ \vdots \\ f_{imaginary}(x_N,y_N) \end{bmatrix}$$

If the inverse Fourier transform F^{-1} is observed as transformation of real and imaginary elements where,

$$F^{-1}_{real}=\left[\left(F^{-1}_{y,real}\otimes F^{-1}_{x,real}\right)-\left(F^{-1}_{y,imaginary}\otimes F^{-1}_{x,imaginary}\right)\right]$$

&

$$F^{-1}_{imaginary}=\left[\left(F^{-1}_{y,real}\otimes F^{-1}_{x,imaginary}\right)+\left(F^{-1}_{y,\mathrm{Im}aginary}\otimes F^{-1}_{x,real}\right)\right]$$

$$O = \begin{bmatrix} F_{real}^{-1} & -F_{imaginary}^{-1} \\ F_{imaginary}^{-1} & F_{real}^{-1} \end{bmatrix}$$

Then the reconstruction of the complex valued *k*-space data $f(x,y)$ can be represented as $v(x,y)$ with dimensions $2N^2 \times 1$,

$$\begin{bmatrix} v_{real}(x_1, y_1) \\ \vdots \\ v_{real}(x_N, y_N) \\ v_{imaginary}(x_1, y_1) \\ \vdots \\ v_{imaginary}(x_N, y_N) \end{bmatrix} = \begin{bmatrix} F_{real}^{-1} & -F_{imaginary}^{-1} \\ F_{imaginary}^{-1} & F_{real}^{-1} \end{bmatrix} \begin{bmatrix} f_{real}(x_1, y_1) \\ \vdots \\ f_{real}(x_N, y_N) \\ f_{imaginary}(x_1, y_1) \\ \vdots \\ f_{imaginary}(x_N, y_N) \end{bmatrix}$$

$$v(x,y) = O \times f(x,y)$$

It should be noted that because *k*-space data is complex-valued, there are both real and imaginary components both of which are essential to reconstruction. However it is (an ill-advised) common practice to discard to imaginary components after reconstruction and continue magnitude only (MO) data in any analysis. From this point on, only MO-images will be used for simplicity, but one should keep in mind that CV-images do have its benefits.

3. Methods

Given the amount of variability in an image registration algorithm, numerous scenarios will be analyzed for a better understanding of its effects. These scenarios will be chosen to stress the difference between a Monte Carlo and the Linear Framework model, the independent statistical effects of image registration algorithms, and the compounded statistical effects of image registration algorithms and other image processing algorithms. It is emphasized that these scenarios are not chosen to produce the highest quality image registration results. Before specifying the scenarios, several aspects of an image registration algorithm will be elaborated upon; once again, the two main steps will be discussed independently.

3.1. Geometric Transformation

In these experiments the quality of the image registration itself is secondary, the primary focus is in the statistical effects of the algorithm itself. Computational efficiency is also emphasized over quality, as image registration is generally a very computationally expensive and time consuming process. Keeping this in mind the image algorithm implemented here is considered to be a simplified version of the algorithms found in the previously mentioned software packages; 6 parameters (2 rotations, 2 shifts, and 2 scales) are optimized with respect to the mean squared error (MSE), the MSE is optimized by iteratively searching through the parameters. Parallel computing methods are implemented where possible to further enhance computational efficiency.

3.2. Interpolation Schemes

There are multiple interpolation methods and a full list can be found from each software's respective user guides. A few common ones were selected: (a) nearest neighbor interpolation, (b) full sinc interpolation, and a (c) rectangular windowed sinc interpolation. Each interpolation method will be defined, Eq. 4 (a) – (c), and formulated as a matrix operator, Figs 2 (a) – (f).

Given a reconstructed image $f(x,y)$ of dimension $N \times N$ with non-integer valued spatial coordinates (x,y), Eq. 4(a)

$$v(i,j) = f(x,y) \text{ , if } \arg\min_{x,y} = (\| (x,y) - (i,j) \|), \begin{matrix} i = 1,1,...2,2,...N,N \\ j = 1,2,...1,2...1,2 \end{matrix}$$

Given a reconstructed image $f(x,y)$ of dimension $N \times N$ with non-integer valued spatial coordinates (x,y), Eq. 4(b)

$$v(i,j) = \sum_{a=1}^{N} \sum_{b=1}^{N} f(x,y) \text{sinc}(x-a) \text{sinc(y-b)}$$

Given a reconstructed image $f(x,y)$ of dimension $N \times N$ with non-integer valued spatial coordinates (x,y), and a rectangular window of length w, Eq. 4(c)

$$v(i,j) = \begin{cases} \sum_{a=i-\frac{w-1}{2}}^{i+\frac{w-1}{2}} \sum_{b=j-\frac{w-1}{2}}^{j+\frac{w-1}{2}} f(x,y) \text{sinc}(x-a) \text{sinc}(y-b), \text{ if } w \bmod 2 = 1 \\ \sum_{a=i-\frac{w}{2}}^{i+\frac{w}{2}} \sum_{b=j-\frac{w}{2}}^{j+\frac{w}{2}} f(x,y) \text{sinc}(x-a) \text{sinc}(y-b), \text{ if } w \bmod 2 = 0 \end{cases}$$

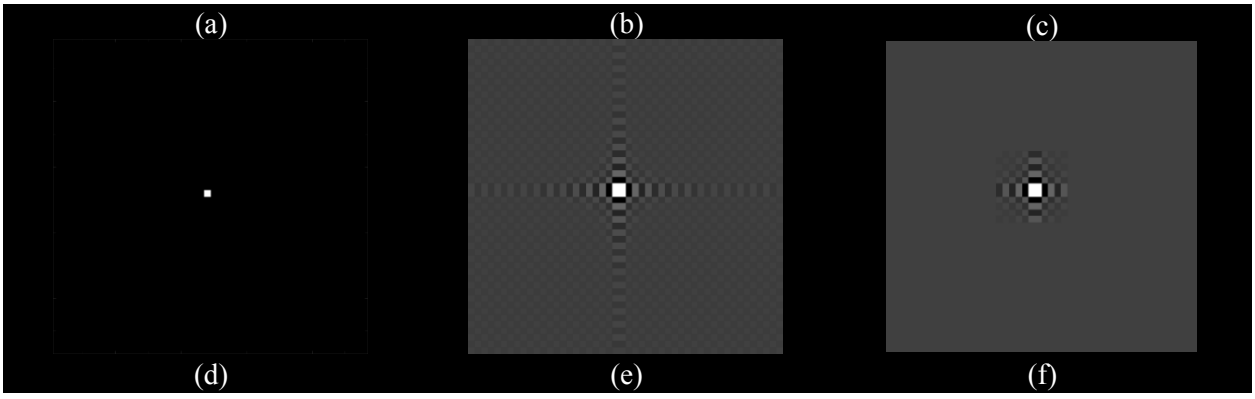

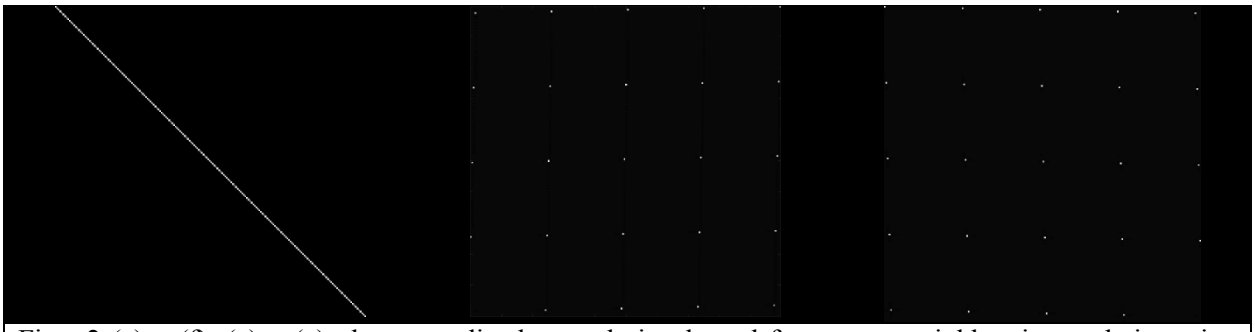

Figs. 2 (a) – (f). (a) – (c), the generalized convolution kernel for nearest neighbor interpolation, sinc interpolation, and windowed sinc interpolation. (d) – (f), the first 200×200 elements of a generalized matrix operator for nearest neighbor interpolation, sinc interpolation, and windowed sinc interpolation.

4. Results

4.1. Experimental Design

The data set was collected from the General Electric 3.0 T Signa LX Magnetic Resonance Imager at the Medical College of Wisconsin. The scan was obtained at an oblique orientation with a single channel coil without RAMP sampling, the dimensions of the image are 96 voxels × 96 voxels × 11 slices with a 24 cm field of view. The timing parameters of the image were as follows: 1 second Time to Repetition (TR) totaling at 720 TRs and 38.5 ms Time to Echo (TE). The tasks of the scan included a block design motor bi-lateral finger tapping with 9 second alternating periods, a block design visual flashing checkerboard 16 second alternating periods, and periodic turning of the head in order to induce motion.

The raw data set with no processing was used in order to enhance the validity of our results. The only preprocessing implemented was a Nyquist ghost correction in order to compensate for an aliasing artifact which would not induce correlation from uncorrelated data. The intention was to minimize the number of other processing steps in order to isolate the effects of registration algorithms. The template chosen was TR image 360, and the slice to be registered is TR image 720, as displayed in Fig. 3.

Several scenarios will be presented and examined. Once again, these scenarios will be chosen to highlight the difference between a Monte Carlo simulation and the Linear Framework theoretical model, and the independent statistical effects of image registration The parameters were also chosen with the aforementioned goals in mind and are described in Table 1. The simulations were implemented with 1000 trials and the addition of noise with a normal distribution of mean, 0, and standard deviation, 0.1.

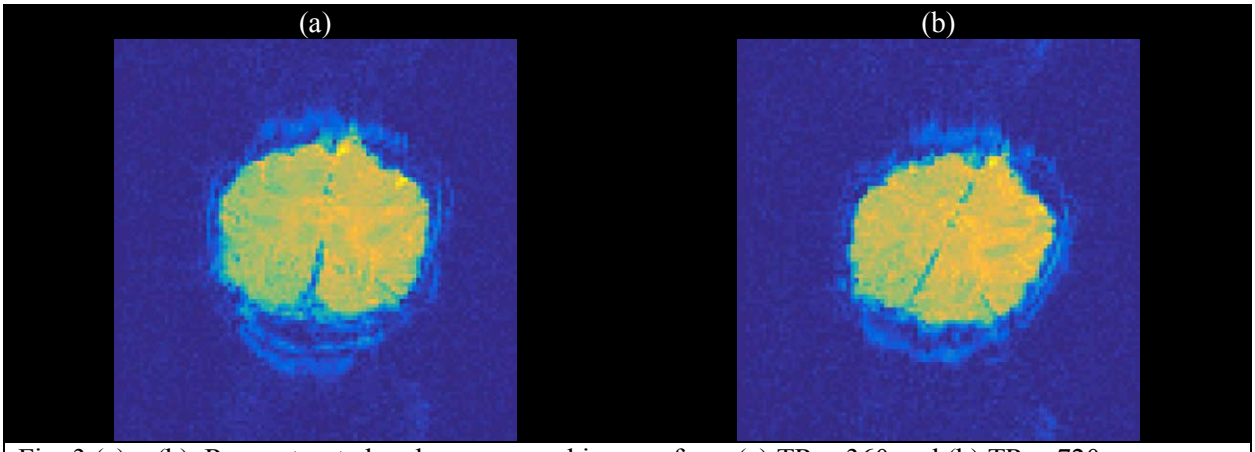

Fig. 3 (a) – (b). Reconstructed and unprocessed images from (a) TR = 360 and (b) TR = 720.

Table 1. List of parameters in each scenario. No Parameters represents scenarios which do not require specification and N/A represents scenarios that are not analyzed.

	No Processing	**Gaussian Smoothing**	**Nearest Neighbor**	**Full Sinc**	**Rectangular windowed Sinc**
Monte Carlo Simulation	Sc. 1 (a): No Parameters	Sc. 1 (b): Full Width at Half Maximum = 3 Voxels	N/A	N/A	N/A
Framework Theoreticaal	Sc. 2 (a): No Parameters	Sc. 2 (b): Full Width at Half Maximum = 3 Voxels	Sc. 2 (c): No Parameters	Sc. 2 (d): No Parameters	Sc. 2 (e): Rectangular window length = 11 voxels

4.2. Statistical Analysis

For each scenario a covariance matrix, correlation matrix, and the correlation of a particular voxel and every other will be examined. The collected data set is a time series of images, but for now only the spatial statistical effects are examined and the temporal effects are excluded. The covariance matrices are structured such that the diagonal elements are the variance of each voxel, and the rows or columns are the covariance of one voxel and all others. The correlation matrices are structured such that the diagonal elements are 1's, and the rows or columns are the correlation of one voxel and all others. The results of Sc. 1 (a) – (b) will be presented first, Figs. 4 (a) – (f), followed by the results of Sc. 2 (a) – (f), Figs. 5 (a) – (f), Figs 6 (a) – (f), & Figs 7 (a) – (f).

The aforementioned noise included in Monte Carlo simulations becomes abundantly clear; even at 1000 trials it is problematic. In statistics a heuristic rule is that you want 10 times more observations than parameters estimated. In the covariance matrix there are $4N^2$ elements which means there are $4N^2$ $(4N^2+1)/2$ unique covariance parameters not including any mean parameters. In Fig. 5 (f), it is obvious that Gaussian smoothing induces a locally radial correlation, but the shape and specificity are lacking. Fig. 7 (b) displays the same Gaussian smoothing under the linear framework model, without the same noisy effects.

Without any processing one can expect no induced correlations, but even with processing not all have an effect as seen with nearest neighbor interpolation in Fig. 5,6,7 (c). The structure and intensity of these effects are a reflection of the respective processing techniques. This is most obvious with the Gaussian smoothing and sinc interpolation, both are similar in structure to their respective convolution mask, Figs 7 (b), (d). In addition, the structure of the sinc interpolation could be change with a rectangular window.

5. Discussion

It is well known that there can be statistical implication from image processing techniques, but it should not be accepted as an uncontrollable condition of working with experimental data. Although there is access to a great number of data sources now, understanding what is happening to the data is just as important. Aside from a greater awareness of the problem at hand, this linear framework will attribute to a better understanding of the individual processing techniques. These alterations in statistical parameters of a data set can lead to inaccurate conclusions. Quantifying will be the first steps in developing future models which will account for such alterations.

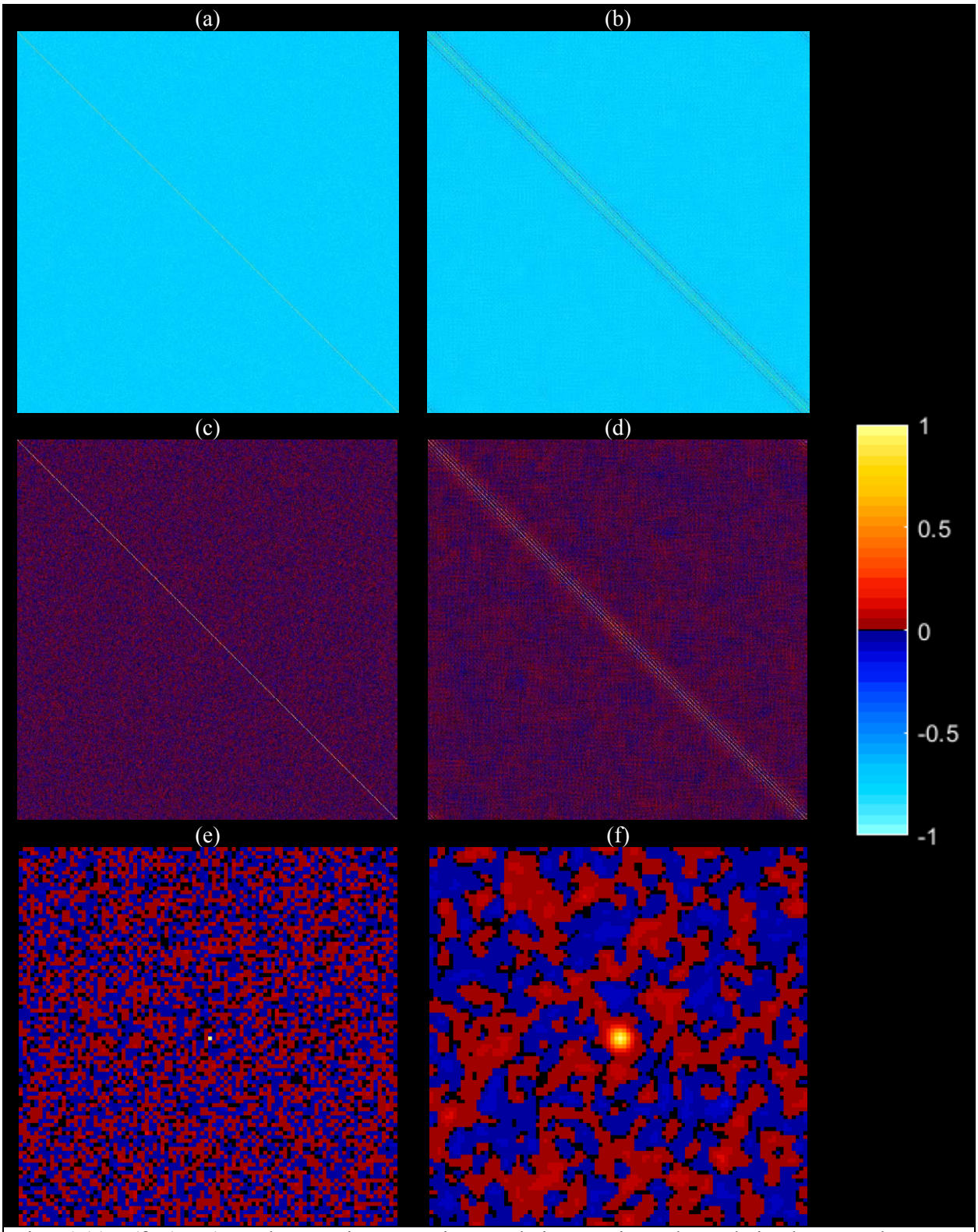

Figs. 4 (a) – (f). (a,c,e) are the covariance matrix, correlation matrix, and correlation between the center voxel and all others of Sc. 1 (a). (b,d,f) are the covariance matrix, correlation matrix, and correlation between the center voxel and all others of Sc. 1 (b).

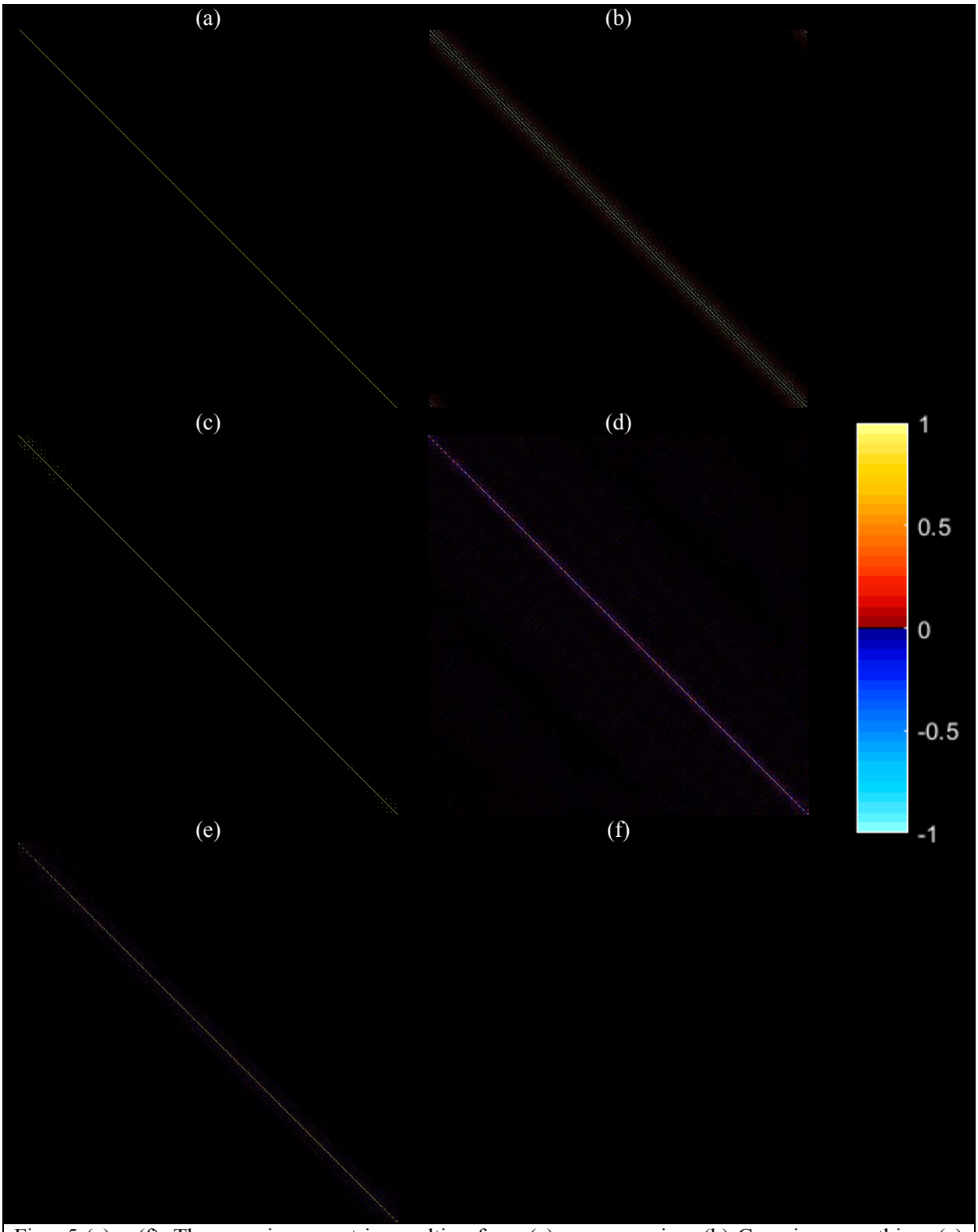

Figs. 5 (a) – (f). The covariance matrix resulting from (a) no processing, (b) Gaussian smoothing, (c) nearest neighbor interpolation, (d) full sinc interpolation, and (e) rectangular windowed sinc interpolation.

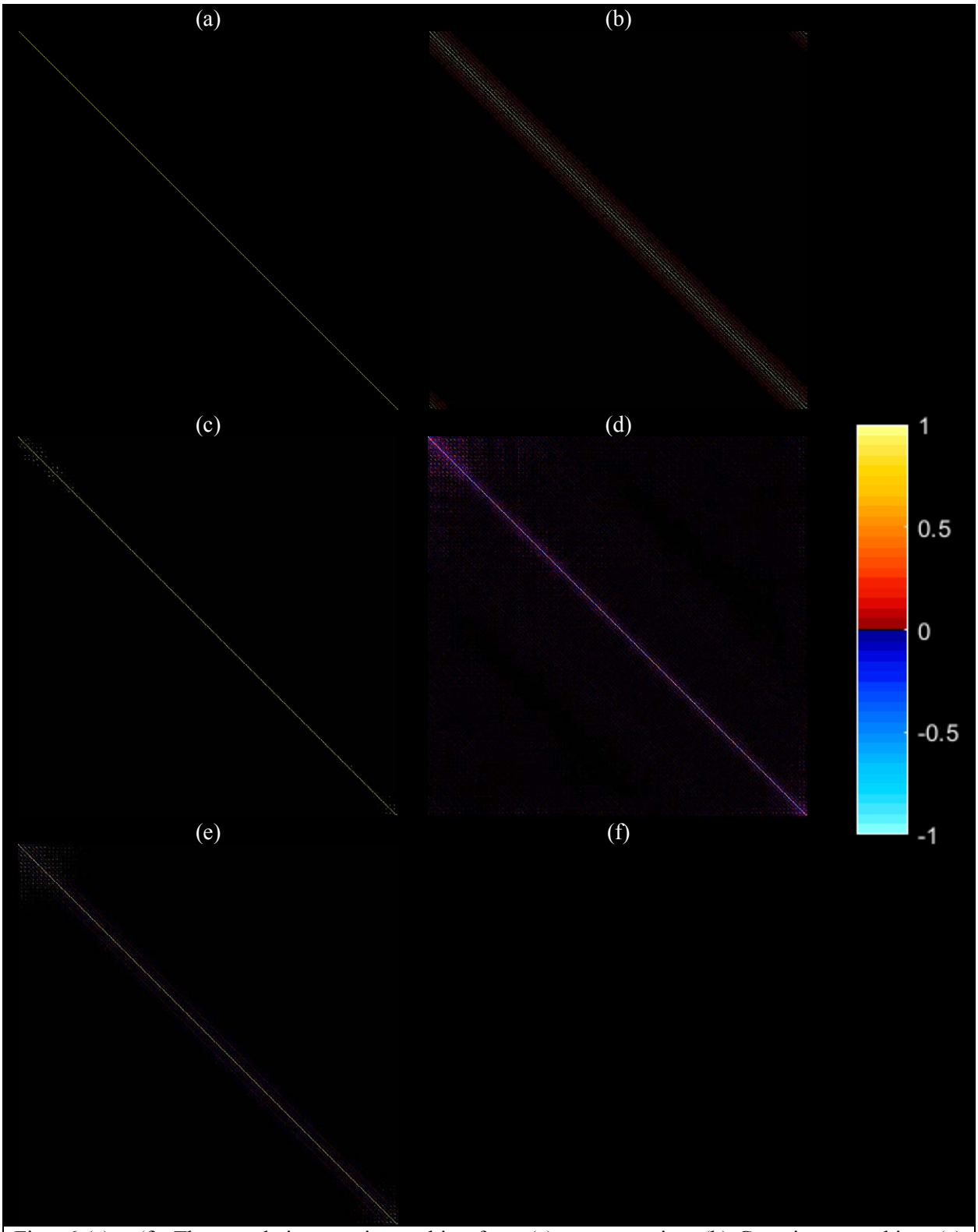

Figs. 6 (a) – (f). The correlation matrix resulting from (a) no processing, (b) Gaussian smoothing, (c) nearest neighbor interpolation, (d) full sinc interpolation, and (e) rectangular windowed sinc interpolation.

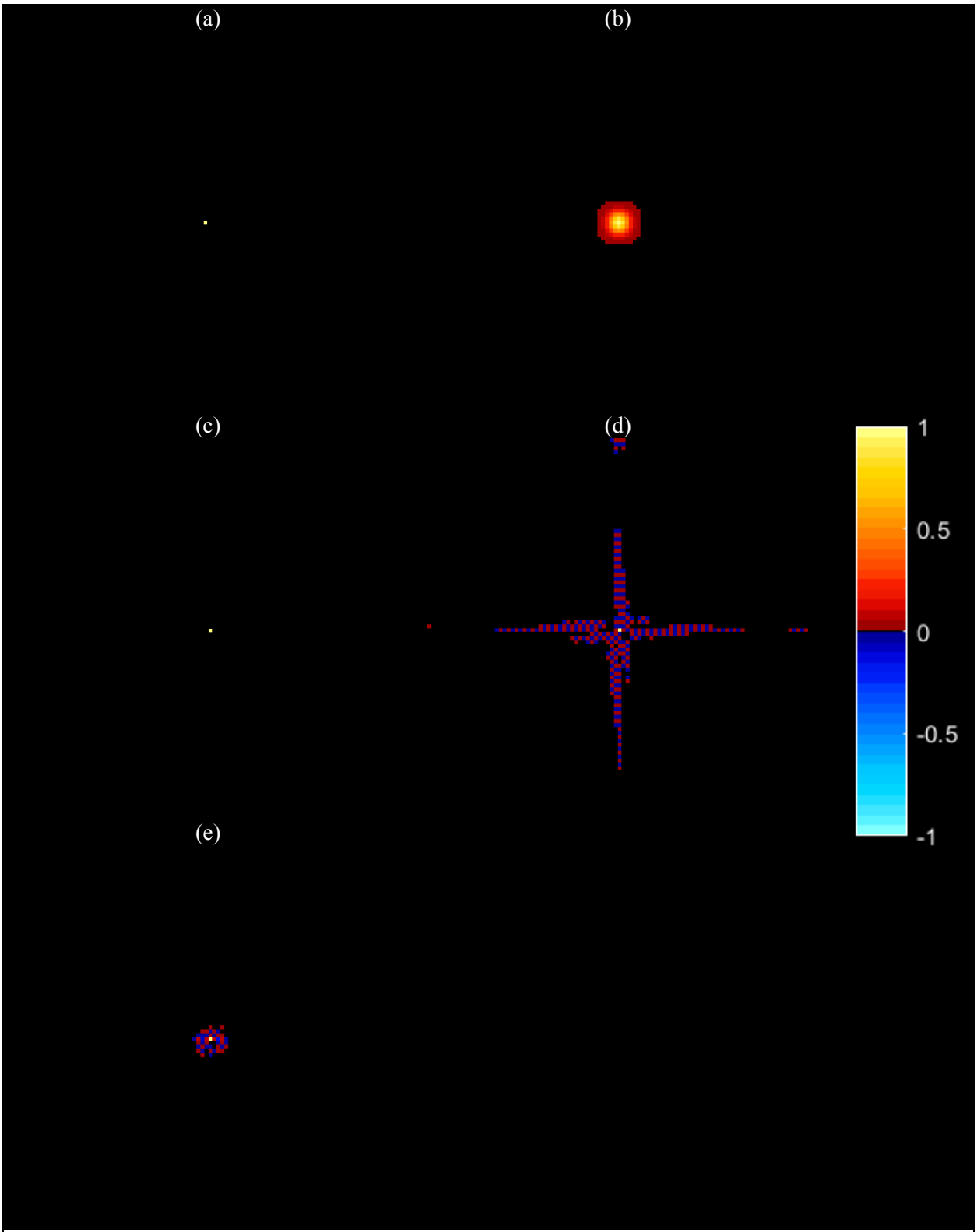

Figs. 7 (a) – (f). The correlation between voxel at spatial location (49,49) and all others resulting from (a) no processing, (b) Gaussian smoothing, (c) nearest neighbor interpolation, and (d) full sinc interpolation, (e) rectangular windowed sinc interpolation.

References

This work was supported by National Institutes of Health research grant R21NS087450.

[1] Ashburner, J., and K. Friston. "Rigid Body Registration". *Statistical Parametric Mapping* (2007): 49-62. Web. 13 Apr. 2016.

[2] Ashburner, John, and Karl J. Friston. "Nonlinear Spatial Normalization Using Basis Functions". *Human Brain Mapping* 7.4 (1999): 254-266. Web.

[3] Bookstein, F.L. "Principal Warps: Thin-Plate Splines And The Decomposition Of Deformations". *IEEE Transactions on Pattern Analysis and Machine Intelligence* 11.6 (1989): 567-585. Web. 13 Apr. 2016.

[4] Buhmann, M. D. *Radial Basis Functions*. Cambridge: Cambridge University Press, 2003. Print.

[5] Friston, Karl. J. et al. "Spatial Registration And Normalization Of Images". *Human Brain Mapping* 3.3 (1995): 165-189. Web. 13 Apr. 2016.

[6] Gianluca, Donato, and Serge Belongie. "Approximate Thin Plate Spline Mappings". *Proceedings of the 7th European Conference on Computer Vision-Part III (ECCV '02)* (2002): 21-31. Print.

[7] Jenkinson, Mark, and Stephen Smith. "A Global Optimisation Method For Robust Affine Registration Of Brain Images". *Medical Image Analysis* 5.2 (2001): 143-156. Web.

[8] Karaman, Muge et al. "Quantification Of The Statistical Effects Of Spatiotemporal Processing Of Nontask Fmri Data". *Brain Connectivity* 4.9 (2014): 649-661. Web.

[9] Nencka, Andrew S., Andrew D. Hahn, and Daniel B. Rowe. "A Mathematical Model For Understanding The Statistical Effects Of K-Space (AMMUST-K) Preprocessing On Observed Voxel Measurements In Fcmri And Fmri". *Journal of Neuroscience Methods* 181.2 (2009): 268-282. Web. 13 Apr. 2016.

[10] Rowe, Daniel B., Andrew S. Nencka, and Raymond G. Hoffmann. "Signal And Noise Of Fourier Reconstructed Fmri Data". *Journal of Neuroscience Methods* 159.2 (2007): 361-369. Web. 13 Apr. 2016.